Formation of interstellar 2,4-pentadiynylidyne, HCCCCC($X\,^2\Pi$), via the neutral-neutral reaction of ground state carbon atom, C(^3P), with diacetylene, HCCCCH($X\,^1\Sigma_g^+$)

B. J. Sun,[1] C. Y. Huang,[1] H. H. Kuo,[1] K. T. Chen,[1] H. L. Sun,[1] C. H. Huang,[1] M. F. Tsai,[1] C. H. Kao,[1] Y. S. Wang,[1] L. G. Gao,[1] R. I. Kaiser,[2] and A. H. H. Chang[1,a)]
[1]*Department of Chemistry, National Dong Hwa University, Shoufeng, Hualien 974, Taiwan, People's Republic of China*
[2]*Department of Chemistry, University of Hawaii at Manoa, Honolulu, Hawaii 96822, USA*

(Received 29 October 2007; accepted 8 April 2008; published online 23 June 2008)

The interstellar reaction of ground-state carbon atom with the simplest polyyne, diacetylene (HCCCCH), is investigated theoretically to explore probable routes to form hydrogen-deficient carbon clusters at ultralow temperature in cold molecular clouds. The isomerization and dissociation channels for each of the three collision complexes are characterized by utilizing the unrestricted B3LYP/6-311G(d,p) level of theory and the CCSD(T)/cc-pVTZ calculations. With facilitation of RRKM and variational RRKM rate constants at collision energies of 0–10 kcal/mol, the most probable paths, thus reaction mechanism, are determined. Subsequently, the corresponding rate equations are solved that the evolutions of concentrations of collision complexes, intermediates, and products versus time are obtained. As a result, the final products and yields are identified. This study predicts that three collision complexes, c1, c2, and c3, would produce a single final product, 2,4-pentadiynylidyne, HCCCCC($X\,^2\Pi$), C_5H (p1)+H, via the most stable intermediate, carbon chain HC_5H (i4). Our investigation indicates the title reaction is efficient to form astronomically observed 2,4-pentadiynylidyne in cold molecular clouds, where a typical translational temperature is 10 K, via a single bimolecular gas phase reaction. © *2008 American Institute of Physics*. [DOI: 10.1063/1.2918367]

I. INTRODUCTION

More than 130 molecules have been detected in the interstellar medium and circumstellar envelope of carbon stars, among which the carbon chain molecules allocate a significant share.[1] In particular, the largest interstellar molecule,[2] $HC_{11}N$, belongs to the carbon chain closed-shell cyanopolyyne family, in which $HC_{2n+1}N$ ($n=1-5$) have been observed.[12–15] Eight polar C_nH ($n=1-8$) radicals are detected[3–10] in dark molecular clouds among other astronomical sources via radioastronomy, a major methodology in discovering new species. Lack of permanent electric dipoles and thus pure rotational spectra, two polyynes, HC_4H and HC_6H, are tentatively assigned[11] in planetary nebulae via infrared spectroscopy, and none of the odd series, $HC_{2n+1}H$ ($n=1,2\ldots$), is detected in space. Hitherto unobserved symmetric HC_nH molecules are believed to be present in the regions where their derivatives are found. Three cumulene carbenes, H_2C_3, H_2C_4, and H_2C_6, of which the latter two are notably high energy isomers of polyynes, have been readily observed[16–18] by radio telescope owing to their polarity.

The diffuse interstellar bands (DIBs), hundreds of absorption lines in visible regions, is an unsolved mystery in astrophysical spectroscopy.[19] Carbon chain molecules, including C_n, and their ions have long been considered[20,21] as carriers of DIBs. For eight decades since the discovery[27] of DIBs, no definite matches have been found for a single molecule, perhaps with exception of C_7^-,[22] whose assignment is not without disputes.[23,24] The would-be matched molecules are speculated to be in size of 10–50 atoms.[25,26] The famed puzzle unleashes intense laboratory investigations for the electronic absorption spectra of carbon chain molecules in gas phase: for instance, $HC_{2n}H$ up to impressively long $HC_{26}H$,[28] the more reactive $HC_{2n+1}H$ ($n=3-6,9$),[29–31] C_nH[32–35] up to $n=10$ with the electronic transition of C_4H[36] measured by laser induced fluorescence, and even the most recent, protonated polyynes, $HC_{2n}H_2^+$ ($n=3,4$).[37]

As microwave, infrared, and electronic spectroscopy serves to establish the presence and abundance of astronomical molecules, chemical models[38–41] are proposed to explain the observed abundances and at the same time predict likely molecules not yet identified. The reactions[42,43] between the ubiquitous atomic carbon and unsaturated hydrocarbons are thought to be important synthetic routes to complex molecules in interstellar medium. Hence, the prototype C(^3P) $+C_2H_2$ reaction[44,45] has been intensively studied experimentally and theoretically. This reaction of carbon atom with the first member of polyynes, $HC_{2n}H$ ($n=1$) could also be viewed as a mechanism for the formation of $C_{2n+1}H$ ($n=1$) and $HC_{2n+1}H$ ($n=1$) isomers, even C_{2n+1} ($n=1$), and the depletion of the smallest polyyne. It opens a reaction class of $C(^3P)+HC_{2n}H \rightarrow HC_{2n+1}H \rightarrow C_{2n+1}H+H$, and the reaction next in line is simply $C(^3P)+HC_4H \rightarrow HC_3H \rightarrow C_5H+H$. Diacetylene molecules presumably are present in the same in-

a)Electronic mail: hhchang@mail.ndhu.edu.tw. FAX: +886-3-8633570.

terstellar sources where C atoms and C_5H are observed such as dark molecular clouds, which makes the reaction highly probable. HC_5H is conspicuously missing from the list of which gas phase electronic spectra have been measured[30,31] in the laboratory. Incidentally, though synthesized[46,47] in the laboratory, its isomer H_2C_5, a cumulene carbene, has also not been identified in space, while the adjacent members, H_2C_4 and H_2C_6, are observed.[17,18] *Ab initio* calculations have been performed on the singlet,[48,49] triplet,[49–55] and excited[53,54] triplet states of HC_5H, and various isomers[48–53,56] mostly in singlet state. Likewise, theoretical investigation have been carried out for linear[48,52,57–61] C_5H, isomers,[52,59–61] and their electronic excited states.[61]

While previous theoretical efforts mainly target the properties of individual molecules, in this work, a theoretical study is carried out for the reaction of $C(^3P)+HCCCCH(X\ ^1\Sigma_g^+)$, in which intricate interplays among interstellar molecules, HC_5H, C_5H, and their isomers, are expected to constitute its reaction mechanism. Our aim is to identify the exoergic channels without entrance barrier through *ab initio* calculations, which would be relevant to the environments of ultralow temperature and density in dense interstellar clouds, in particular, to derive the reaction mechanism by further computing the rate constants of elementary steps specifically tuned for the condition of single binary collision, to obtain concentration evolutions with time for intermediates and products during the reaction by solving the rate equations of the mechanism, and to predict the product abundances at different collision energies.

There are multiple π systems in diacetylene molecule as vinyl cyanide[62] and cyanoacetylene[63] previously treated in our group, for instance. When attacked by carbon atoms, it is expected to yield multiple collision complexes, and the amount of each collision complex generated would be determined by the bimolecular rate constant for the binary collision between carbon atoms and diacetylenes. Fundamentally, the estimation for the bimolecular rate constant of a barrierless reaction is known to be a particularly challenging task when it is explicitly orientation dependent and multidimensional as for the title reaction of seven-atomic system. In this work, a scheme is devised based on Langevin model[64] to attain the ratio for the cross sections forming multiple collision complexes, respectively, when the reaction is barrierless.

II. THEORETICAL METHODS

A. *Ab initio* electronic structure calculations: Reaction paths prediction

The $C(^3P)+HCCCCH(X\ ^1\Sigma_g^+)$ reaction is assumed to proceed on the adiabatic triplet ground-state potential energy surface of C_5H_2. Possible collision complexes are identified; subsequently, low-energy isomerization channels for each collision complex including hydrogen migration, carbon migration, cyclization, ring opening, and H-atom dissociation are sought and characterized. The optimized geometries and harmonic frequencies of intermediates, transition states, and dissociation products are obtained at the level of the hybrid density functional theory, the unrestricted B3LYP (Ref. 65)/6-311G(d,p), with energies further refined by the coupled cluster[66] CCSD(T)/cc-pVTZ with unrestricted B3LYP/6-31lG(d,p) zero-point energy corrections. The locations of transition state geometries for $C(^3P)+HCCCCH(X\ ^1\Sigma_g^+)$ reaction that lead to the collision complexes are facilitated by intrinsic coordinate calculations (IRC) at unrestricted B3LYP/6-311G(d,p) level of theory along the breaking C–C bonds of respective collision complexes. The GAUSSIAN98 and GAUSSIAN03 programs[67] are employed for the electronic structure calculations.

B. RRKM rate constant calculations

If reaction occurs when the energy equilibration among molecular degrees of freedom has completed, the rate of reaction could be realized statistically. Moreover, provided that the energy is conserved during the course of reaction such as in low-density environments or molecular beam experiments where condition for single collision is achieved, the rate constant could be predicted by utilizing RRKM theory. According to the RRKM theory, for a unimolecular reaction

$$A^* \xrightarrow{k} A^{\neq} \rightarrow P,$$

where A^* is the energized reactant, $A^{\neq}$ represents the transition state, and P the products, the rate constant $k(E)$ at total energy E may be expressed as follows:

$$k(E) = \frac{\sigma}{h}\frac{W^{\neq}(E-E^{\neq})}{\rho(E)}, \tag{1}$$

where σ is the symmetry factor, $W^{\neq}$ the number of states of the transition state, $E^{\neq}$ the transition state energy, and ρ the density of states of the reactant. In this work, ρ and $W^{\neq}$ are computed by saddle-point method,[68,69] molecules are considered as collections of harmonic oscillators, and the harmonic frequencies of which are obtained as described in Sec. II A.

C. Variational RRKM rate constant calculations

If the reactions are reversible, carbon dissociations of the collision complexes back to the reactants, $C(^3P)+HCCCCH$, are expected to be also barrierless as their reversed, the formations of collision complexes. When the straightforward choice of transition state at the top of potential-energy barrier cannot be accomplished in case of a barrierless reaction as such, its kinetic equivalence, the geometry of minimum flux, could be adopted. Namely, instead, the variational transition state is located when (e.g., Refs. 70–72)

$$\frac{\partial W(E,R)}{\partial R} = 0, \tag{2}$$

where W is the number of states and R the reaction coordinate, breaking C–C bond. The variational transition states thus determined would be both energy and reaction coordinate dependent. The IRC calculations for optimized geometries and harmonic frequencies as function of the reaction coordinate for each collision complex dissociating back to reactants are performed at the level of B3LYP/6-311G(d,p). Once the transition state is variationally decided for each

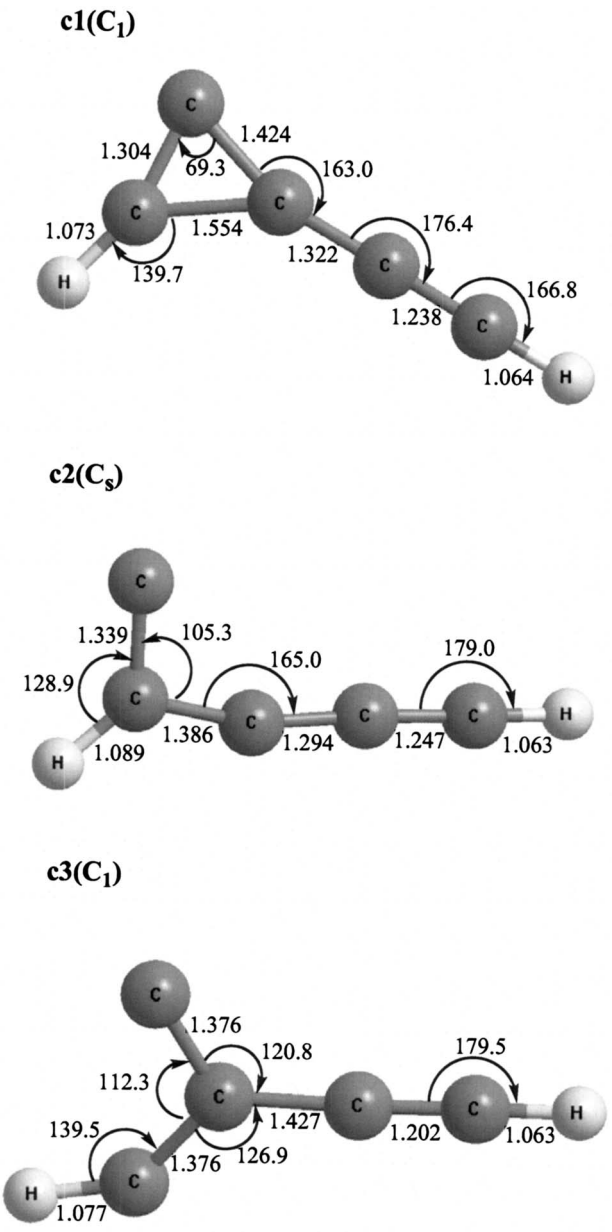

FIG. 1. The B3LYP/6-311G(d,p) optimized geometries of the three collision complexes of the $C(^3P)+HCCCCH(X\ ^1\Sigma_g^+)$ reaction, in which the point group is in parenthesis, lengths in angstroms, and the angles in degrees.

collision complex at each of the six collision energies (0.0, 0.03, 0.15, 2.0, 5, and 10 kcal/mol, which correspond to average kinetic energies of an ideal gas molecule at temperatures of 0, 10, 50, 671, 1678, and 3355 K, respectively.), the CCSD(T)/cc-pVTZ energy is then computed and the RRKM rate constant $k(E)$ of collision complex $\rightarrow C(^3P)+HCCCCH$ could be estimated according to Eq. (1).

D. Solution of the rate equations and branching ratios

The rate equations for reaction mechanism of each collision complex are solved numerically by the Runge–Kutta method at collision energies of 0 and 10 kcal/mol. The solutions yield the concentrations of species in the reaction mechanisms as a function of time. The branching ratios or yields when the reaction is completed could be obtained by taking the asymptotic values.

E. Reaction cross sections for forming collision complexes

With the branching ratio resolved within mechanism of each collision complex as explained in Sec. II D, the branching ratio for the title reaction could then be settled when the reaction cross sections for forming all collision complexes are also known. For a barrierless bimolecular reaction, the intermolecular potential between reactants is often approximated by its long-range form, $V(R)=-C/R^s$, where $s=6$ when both reactants are nonpolar, C is a constant, and R the distance between centers of mass of two reactants, and the simple Langevin model gives the capturing cross section $\sigma(E)\propto(C/E)^{1/3}$, where E is the collision energy. However, the fact that there are multiple collision complexes for the C+HCCCCH reaction clearly indicates the reaction cross section for this bimolecular reaction is utterly orientation dependent, hence cannot be viewed as merely depending on distance. Fundamentally, the cross section is closely related to the potential energy surface; the latter would have to be understood for the cross section to be materialized. For a seven-atomic system in general, the potential energy surface is a formidable 15-dimensional function of nuclear coordinates or internal degrees of freedom. The task to map quantum mechanically even a portion of the 15-dimensional surface is still daunting, in fact, unpractical nowadays.

It would be a logical and sensible alternative in this case to find a reaction coordinate such that the one-dimensional potential curve born out of it could grasp the essence of reaction, and at once drastically reduce the 15-dimensional problem into a manageable one dimension. Admittedly, extracting a "reaction coordinate" is often extremely difficult if not impossible without an educational guess. Instead of aimlessly wondering through the entrance surface of C and HCCCCH collision, we turn to the collision complexes, and let the reaction coordinates be the breaking C–C bonds of respective collision complex's C dissociations, with the hypothesis of the C-dissociation reactions being reversible. One-dimensional potential energy curves, V_1, V_2, and V_3, along thus defined reaction coordinates, R_1, R_2, and R_3, of C+HCCCCH $\rightarrow$ collision complex 1, C+HCCCCH $\rightarrow$ collision complex 2, and C+HCCCCH $\rightarrow$ collision complex 3, respectively, are obtained by the same IRC calculations described in Secs. II A and II C. The asymptotic portions of $V_1(R_1)$, $V_2(R_2)$, and $V_3(R_3)$ are subsequently least square fitted into $-C(1)/R_1^6$, $-C(2)/R_2^6$, and $-C(3)/R_3^6$ to obtain constants, $C(1)$, $C(2)$, and $C(3)$, respectively. If Langevin model is complied, it follows that the ratio of cross sections forming collision complexes would simply be $\sigma_{c1}:\sigma_{c2}:\sigma_{c3}=C(1)^{1/3}:C(2)^{1/3}:C(3)^{1/3}$.

III. RESULTS AND DISCUSSION

The $C(^3P)+HCCCCH(X\ ^1\Sigma_g^+)$ reaction is presumably initiated by the addition of electrophilic carbon atom to the π

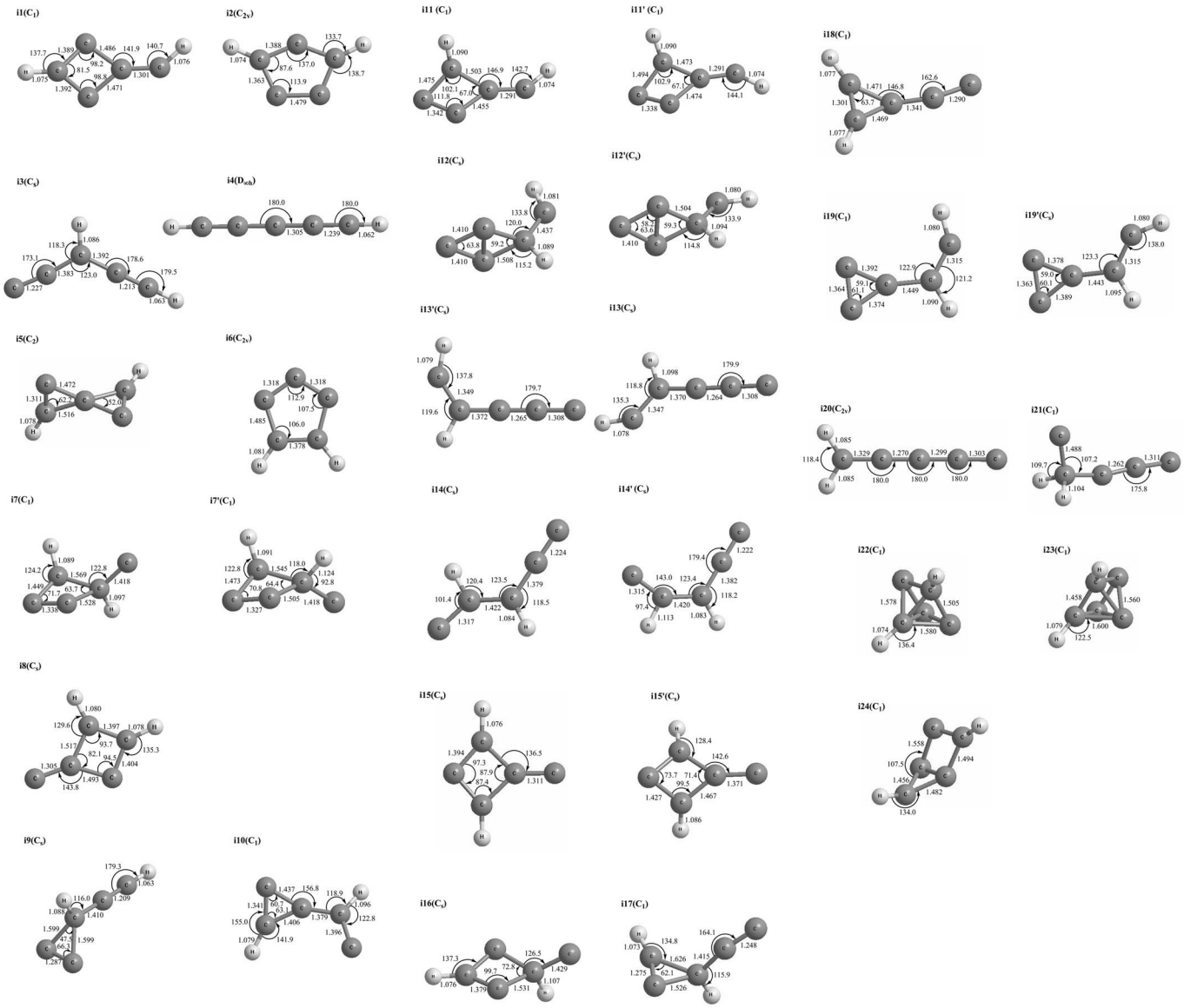

FIG. 2. The B3LYP/6-311G(d,p) optimized geometries of the intermediates for the $C(^3P)+HCCCCH(X\ ^1\Sigma_g^+)$ reaction on the adiabatic triplet ground state potential energy surface of C_5H_2, in which the point group is in parenthesis, the lengths in angstroms, and the angles in degrees.

systems of diacetylene molecule. For a symmetric HCCCCH, there could be three possible collision complexes. The B3LYP/6-311G(d,p) optimized geometries of the resulting three collision complexes, denoted c1(ethynylcyclopropenylidene), c2(pent-4-ene-5, 5-diyl-1,2-diyne), and c3(2-ethynyl-allene-1-yl-3-ylidene), are illustrated in Fig. 1.

Each binary collision event of reactants, $C(^3P)$ and $HCCCCH(X\ ^1\Sigma_g^+)$, could yield only one of these three collision complexes. It would be logical therefore that the reaction paths of the titled reaction are mapped out by following the routes for individual collision complex. The immediate channels of c1, c2, and c3, respectively, are probable low-energy isomerizations including hydrogen shift, carbon shift, ring formation, ring opening, carbon decomposition, and hydrogen dissociation, of which the isomers (or intermediates) and corresponding transition states are characterized if proven plausible. The rate constants for all the immediate paths with energy under 10 kcal/mol relative to the reactants are then estimated. A simple scheme is adopted to sensibly avoid escalating number of possible pathways: only the immediate channels for those intermediates of the largest rate constants, or equivalently along the most kinetically competitive paths, are tracked further. The B3LYP/6-311G(d,p) optimized structures of intermediates, H-dissociation products, and transition states, designated as i, p, and ts, are drawn in Figs. 2, 3, s1,[73] and 4, respectively; their predicted energies are listed in Table sI[73] and the rate constants of elementary steps computed at collision energies of 0.0, 0.03, 0.15, 2.0, 5, and 10 kcal/mol in Table I. The schematic CCSD(T)/cc-pVTZ energetic paths of c1, c2, and c3 thus determined are plotted in Figs. 5–7, respectively. With the criterion being kinetically advantaged, the most

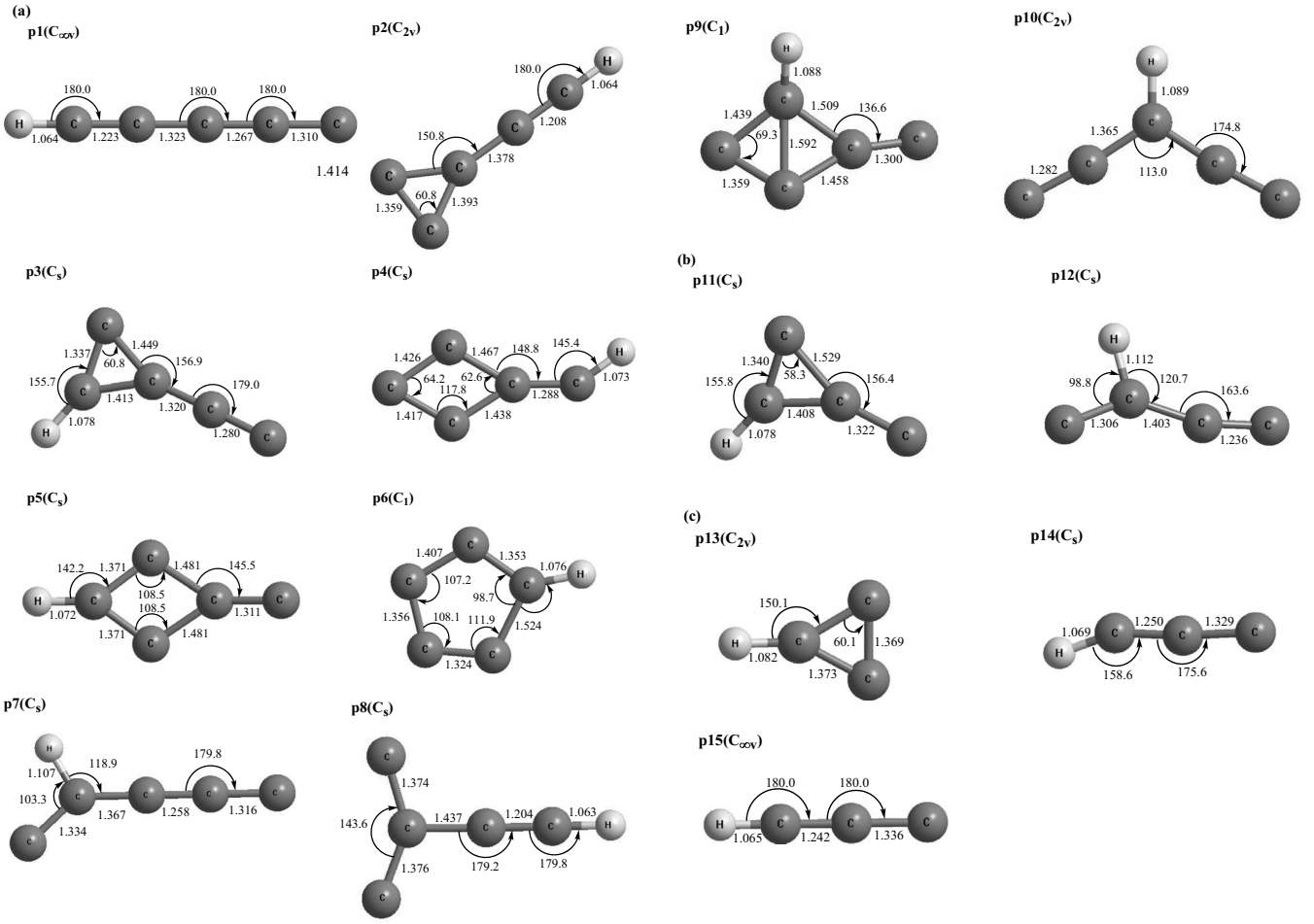

FIG. 3. The B3LYP/6-311G(d,p) optimized geometries of dissociation products for the $C(^3P)+HCCCCH(X\ ^1\Sigma_g^+)$ reaction, in which the point group is in parenthesis, the lengths in angstroms, and the angles in degrees: (a) the hydrogen atom dissociation products, C_5H, in doublet ground states; (b) the CH dissociation products, C_4H, in doublet ground states; (c) the C_2H dissociation products, C_3H, in doublet ground states.

probable paths for c1, c2, and c3 are concluded as presented in Figs. 8–10, respectively. Correspondingly, the reaction mechanisms inferred are drafted in Fig. 11.

Unless otherwise stated, in the discussion that follows, the energies cited are the CCSD(T)/cc-pVTZ energies relative to the reactants with B3LYP/6-311G(d,p) zero-point energy corrections, and the rate constants referred to are at zero collision energy.

A. Dissociation of collision complex back to reactants, C+HCCCCH

All three collision complexes are considerably bound relative to the reactants, by 54.0, 44.2, and 25.4 kcal/mol for c1, c2, and c3, respectively, as tabulated in Table sI. While a singlet c1 is predicted[48,51] of C_s symmetry, the out of plane ethynyl hydrogen makes the present triplet c1 possesses no symmetry. Similarly, an out of plane H atom renders c3 being of C_1 point group, which leaves planar c2 the only symmetrical collision complex.

The energy-dependent transition states, tsc1, tsc2, and tsc3, of carbon dissociations, c1→C+HCCCCH, c2→C+HCCCCH, and c3→C+HCCCCH, respectively, are determined with aids of variational RRKM theory. The transition states at six collision energies (0.0, 0.03, 0.15, 2.0, 5.0, and 10.0 kcal/mol) are searched for each collision complex, which amounts to a total of 18 transition states for c1, c2, and c3. Their geometries in Fig. 4 indicate that the leaving C–C separations fall within 4.1–3.6, 3.9–3.4, and 3.8–3.3 Å for tsc1, tsc2, and tsc3, respectively, as collision energy increases from 0.0 to 10 kcal/mol. It is in line with the expectation that transition state gets tighter (i.e., shorter C–C distance) as available energy grows. The energies are located at −0.7 to −1.2, −0.6 to −1.2, and −1.0 to −1.6 kcal/mol for tsc1, tsc2, and tsc3, respectively, which is reasonable considering the already reactantlike geometries. Now that the three transition state energies are rather close in magnitude, the activation energies in turn predominately depend on the stability of the collision complexes. Thus, c1 would encounter the highest barrier, followed by c2's, and the least stable c3 is most likely to eliminate the carbon atom among the three. The phenomenon is demonstrated nicely by the predicted rate constants in Table I, which precisely take the order of $k_{c1}<k_{c2}<k_{c3}$ through collision energies of 0–10 kcal/mol.

B. Dissociation products

Ten relevant H-dissociation products, C_5H, are listed in Table sI and the geometries displayed in Fig. 3(a). The linear pent-2,3,4-triene-5-ylidene-1-yne (p1) is the most stable, fol-

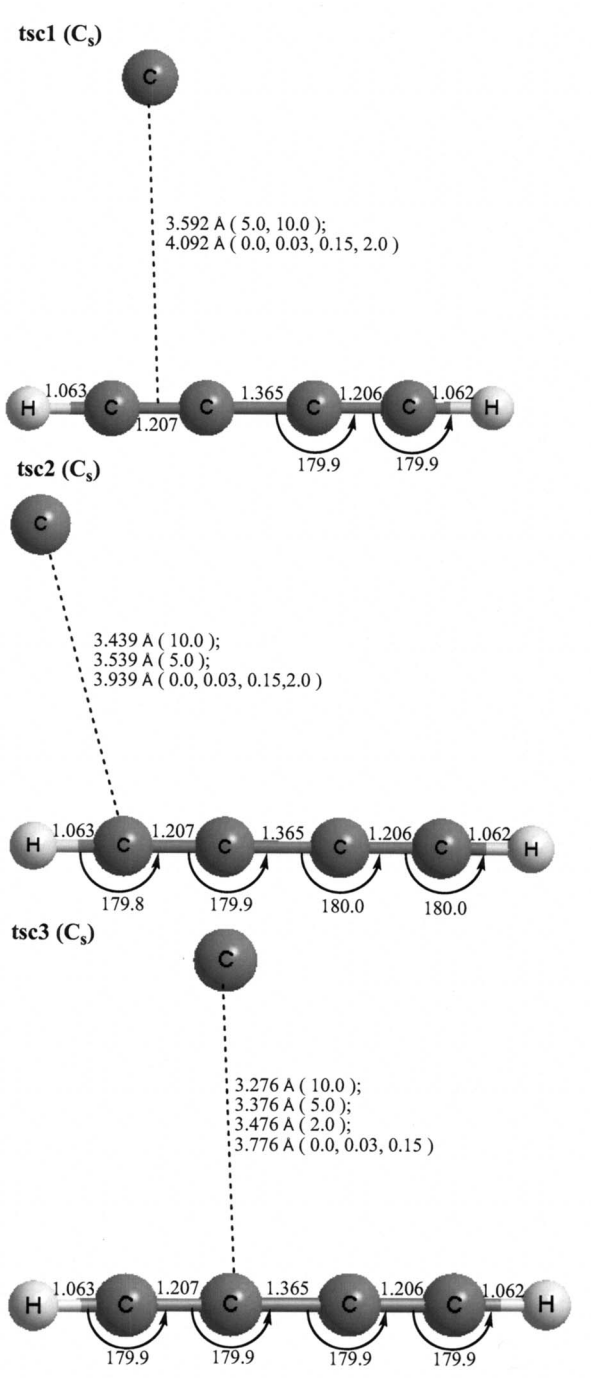

FIG. 4. The schematic B3LYP/6-311G(d,p) geometries of the variationl transition states for carbon decomposition reactions of collision complexes, c1–c3, on the adiabatic triplet ground state potential energy surface of C_5H_2, in which the point group is in parenthesis, the lengths in angstroms, and the angles in degrees. Also, note that the collision energies are specified in the parentheses next to the corresponding breaking CC bond lengths of tsc1–tsc3.

lowed by two three-member ringed cycloprop-1,2,3-triene-1-ethyne (p2) and cycloprop-1,2-dieneyl-ethyne-1-ylidene (p3), and subsequently two four-member ringed but-1-yne-2,3-diene-2,4-diylidenecarbene (p4) and 3-hydrocyclobut-1,2-diene-4-yne-1-ylidenecarbene (p5). The cyclopent-1,2,3,4-tetraene-5-ylidene (p6) of five-member ring is ranked highest in energy. It appears the stability of cyclic C_5H decreases with increasing ring size. Despite the energy of linear carbon chain p1 being the lowest, once the H atom moves away from the terminal carbon to bind instead the second or third C forming nonlinear chained p7 and pent-3-ene-1,4-diyne-1,5-diylidene (p10), respectively, the disruption in delocalization of π electrons could destabilize the molecule significantly by an amount of near 60 kcal/mol as estimated from the energy differences with p1. The energy of a branched carbon chain p8 is stepped up even further.

The energy of p1+H sinks lightly at −9.6 kcal/mol, and the 0.7 kcal/mol of the second most stable p2+H is already not bound compared to the reactants. A distant third, p3+H, is located at 18.1 kcal/mol, and the most unattainable p6 +H, 95.8 kcal/mol, with others scattered in between. With the exception of p1 and, tentatively, p2, energetic concern alone has set the rest of C_5H's squarely out of the picture of low-temperature reaction mechanism. By the same token, the C+HCCCCH as C-dissociation products, in addition to p1, the only products with transition-state energies lower than the reactants, may well be a plausible outcome for the titled reaction energetically. Note that the four-member ringed p5 and 3-hydrobicyclo[1,1,0]but-1,2-diene-4-ylidenecarbene (p9) are newly predicted C_5H isomers in the current investigation; the rest have also been characterized theoretically among various works.[48,52,57–61]

The feasibility of CH and C_2H eliminations is gauged. As grouped in Table sI and Figs. 3(b) and 3(c), the C_2H-dissociation products can only be attained by around 30 kcal/mol; moreover, the products due to CH decomposition are located at 84.7 kcal/mol and beyond. Evidently, these channels are plainly not within reach below the collision energy of 10 kcal/mol and at ultra low temperature.

C. Reaction paths of ethynylcyclopropenylidene (c1)

As seen in Fig. 5, ring opening could lead c1 to pent-1,4-diyne-2,3-diene (i4) and c2 by overcoming barriers of 7.7 and 9.7 kcal/mol, respectively; ring opening to c3, however, does not seem probable since the transition state has not been found. With activation energies of 38.8 and 57.8 kcal/mol, the cyclic c1 could undergo further cyclization to form biringed spiro[2,2]pent-2,5-diyl-1,4-diene (i5) of two three-membered rings, and bicyclo[1,2,0]pent-1,3,4-triene (i24) of three- and four-membered rings at −23.6 and −5.0 kcal/mol, respectively. Possible 1,2 H-shifts in c1 would presumably give cycloprop-2-ynyl-ethyne (i9) and cycloprop-2,3-dienyl-etheneylidene (i10); present calculations prove only the former is feasible with a high barrier of 49.3 kcal/mol. Other than the carbon decomposition back to form the reactants, C+HCCCCH, the most energetically accessible direct dissociation products of c1 are predicted to be p2 and p3 located at still higher 0.7 and 18.1 kcal/mol, respectively, as a result of H elimination. The 7.7 kcal/mol barrier of c1→i4 reaction appears the easiest to conquer, while a close second tsc1c2 is higher by a mere 2 kcal/mol. The paths via tsc1i5, tsc1i9, and tsc1i24 would be very difficult to compete with c1→i4 and c1→c2.

The scenario is made more apparent by the rate constant calculations, which at zero collision energy estimate k_1

TABLE I. The RRKM rate constants (s^{-1}) computed with B3LYP/6-311G(d,p) zero-point energy corrected CCSD(T)/cc-pVTZ energies, and B3LYP/6-311G(d,p) harmonic frequencies at collision energies of 0.0, 0.03, 0.15, 2.0, 5.0, and 10.0 kcal/mol.

	0.0	0.03	0.15	2.0	5.0	10.0
k_{c1} (c1 → C+HCCCCH)	4.42×10^{3}	4.69×10^{3}	5.90×10^{3}	7.81×10^{4}	1.06×10^{6}	1.41×10^{7}
k_{c2} (c2 → C+HCCCCH)	1.0×10^{4}	1.1×10^{4}	1.38×10^{4}	1.86×10^{5}	2.41×10^{6}	3.17×10^{7}
k_{c3} (c3 → C+HCCCCH)	3.66×10^{6}	3.82×10^{6}	4.50×10^{6}	2.80×10^{7}	2.01×10^{8}	1.44×10^{9}
k_{1} (c1 → i4)	7.10×10^{12}	7.10×10^{12}	7.12×10^{12}	7.43×10^{12}	7.93×10^{12}	8.71×10^{12}
k_{-1} (i4 → c1)	7.98×10^{8}	8.00×10^{8}	8.09×10^{8}	9.58×10^{8}	1.24×10^{9}	1.82×10^{9}
k_{2} (c1 → c2)	5.59×10^{11}	5.59×10^{11}	5.61×10^{11}	5.94×10^{11}	6.47×10^{11}	7.34×10^{11}
k_{-2} (c2 → c1)[a]	1.89×10^{12}	1.89×10^{12}	1.89×10^{12}	1.90×10^{12}	1.91×10^{12}	1.92×10^{12}
k_{3} (c1 → i5)	3.54×10^{7}	3.57×10^{7}	3.68×10^{7}	5.76×10^{7}	1.09×10^{8}	2.63×10^{8}
k_{-3} (i5 → c1)	7.73×10^{11}	7.76×10^{11}	7.87×10^{11}	9.69×10^{11}	1.29×10^{12}	1.88×10^{12}
k_{4} (c1 → i9)	9.11×10^{4}	9.31×10^{4}	1.01×10^{5}	3.28×10^{5}	1.47×10^{6}	9.24×10^{6}
k_{-4} (i9 → c1)	2.29×10^{8}	2.33×10^{8}	2.51×10^{8}	7.10×10^{8}	2.59×10^{9}	1.21×10^{10}
k_{5} (c2 → i1)	5.26×10^{10}	5.27×10^{10}	5.30×10^{10}	5.84×10^{10}	6.72×10^{10}	8.24×10^{10}
k_{-5} (i1 → c2)	1.44×10^{13}	1.44×10^{13}	1.45×10^{13}	1.54×10^{13}	1.69×10^{13}	1.93×10^{13}
k_{6} (c2 → i3)	6.12×10^{10}	6.15×10^{10}	6.27×10^{10}	8.29×10^{10}	1.24×10^{11}	2.18×10^{11}
k_{-6} (i3 → c2)	3.56×10^{10}	3.58×10^{10}	3.67×10^{10}	5.29×10^{10}	9.02×10^{10}	1.92×10^{11}
k_{7} (c2 → i2)	4.32×10^{8}	4.33×10^{8}	4.40×10^{8}	5.53×10^{8}	7.69×10^{8}	1.22×10^{9}
k_{-7} (i2 → c2)	2.30×10^{10}	2.31×10^{10}	2.35×10^{10}	3.08×10^{10}	4.55×10^{10}	7.91×10^{10}
k_{8} (c2 → c3)	3.33×10^{7}	3.37×10^{7}	3.51×10^{7}	6.46×10^{7}	1.48×10^{8}	4.40×10^{8}
k_{-8} (c3 → c2)	3.95×10^{9}	3.98×10^{9}	4.10×10^{9}	6.21×10^{9}	1.07×10^{10}	2.14×10^{10}
k_{9} (c3 → i1)	4.79×10^{10}	4.80×10^{10}	4.85×10^{10}	5.55×10^{10}	6.69×10^{10}	8.57×10^{10}
k_{-9} (c1 → c3)	2.21×10^{11}	2.22×10^{11}	2.26×10^{11}	3.04×10^{11}	4.63×10^{11}	8.23×10^{11}
k_{10} (i4 → p1)	1.51×10^{3}	1.56×10^{3}	1.77×10^{3}	1.00×10^{4}	8.53×10^{4}	1.13×10^{6}
k_{11} (i3 → i9)	1.94×10^{9}	1.95×10^{9}	1.99×10^{9}	2.71×10^{9}	4.27×10^{9}	8.16×10^{9}
k_{-11} (i9 → i3)	2.68×10^{12}	2.69×10^{12}	2.71×10^{12}	3.12×10^{12}	3.80×10^{12}	4.99×10^{12}
k_{12} (i3 → p1)	4.82×10^{4}	5.03×10^{4}	5.92×10^{4}	4.77×10^{5}	5.17×10^{6}	7.59×10^{7}
k_{13} (i4 → i6)	8.56×10^{1}	8.69×10^{1}	9.23×10^{1}	2.19×10^{2}	7.27×10^{2}	3.65×10^{3}
k_{-13} (i6 → i4)	1.19×10^{10}	1.20×10^{10}	1.26×10^{10}	2.40×10^{10}	5.69×10^{10}	1.73×10^{11}
k_{14} (i4 → i11)	4.48×10^{3}	4.53×10^{3}	4.69×10^{3}	7.97×10^{3}	1.72×10^{4}	5.15×10^{4}
k_{-14} (i11 → i4)	6.92×10^{12}	6.93×10^{12}	6.96×10^{12}	7.43×10^{12}	8.11×10^{12}	9.10×10^{12}
k_{15} (i11′ → i3)	9.24×10^{11}	9.28×10^{11}	9.45×10^{11}	1.22×10^{12}	1.71×10^{12}	2.62×10^{12}

TABLE I. (*Continued.*)

	0.0	0.03	0.15	2.0	5.0	10.0
k_{-15} (i3→i11′)	8.95×10^{6}	9.05×10^{6}	9.45×10^{6}	1.78×10^{7}	4.32×10^{7}	1.43×10^{8}
k_{16} (i13→i3)	6.98×10^{9}	7.05×10^{9}	7.37×10^{9}	1.37×10^{10}	3.19×10^{10}	9.54×10^{10}
k_{-16} (i3→i13)	1.47×10^{8}	1.49×10^{8}	1.57×10^{8}	3.34×10^{8}	9.49×10^{8}	3.80×10^{9}
k_{17} (i10→c2)	1.20×10^{10}	1.23×10^{10}	1.35×10^{10}	4.20×10^{10}	1.31×10^{11}	3.97×10^{11}
k_{-17} (c2→i10)	1.25×10^{4}	1.30×10^{4}	1.49×10^{4}	8.30×10^{4}	5.76×10^{5}	5.02×10^{6}
k_{18} (i11→i11′)	8.24×10^{12}	8.25×10^{12}	8.29×10^{12}	8.78×10^{12}	9.51×10^{12}	1.06×10^{13}
k_{-18} (i11′→i11)	8.88×10^{12}	8.89×10^{12}	8.92×10^{12}	9.43×10^{12}	1.02×10^{13}	1.12×10^{13}
k_{19} (i11′→i12′)	⋯	⋯	⋯	⋯	⋯	3.39×10^{6}
k_{-19} (i12′→i11′)	⋯	⋯	⋯	⋯	⋯	1.24×10^{8}
k_{20} (i6→i14′)	⋯	⋯	⋯	2.72×10^{6}	3.31×10^{7}	3.84×10^{8}
k_{-20} (i14′→i6)	⋯	⋯	⋯	4.90×10^{7}	3.27×10^{8}	1.70×10^{9}
k_{21} (i6→i13)	2.09×10^{10}	2.11×10^{10}	2.18×10^{10}	3.52×10^{10}	6.79×10^{10}	1.62×10^{11}
k_{-21} (i13→i6)	2.30×10^{8}	2.32×10^{8}	2.39×10^{8}	3.85×10^{8}	7.40×10^{8}	1.75×10^{9}
k_{22} (i2→i3)	4.35×10^{10}	4.37×10^{10}	4.46×10^{10}	6.01×10^{10}	9.27×10^{10}	1.70×10^{11}
k_{-22} (i3→i2)	2.37×10^{8}	2.39×10^{8}	2.44×10^{8}	3.45×10^{8}	5.70×10^{8}	1.16×10^{9}
k_{23} (i3→i15)	8.85×10^{7}	8.92×10^{7}	9.18×10^{7}	1.39×10^{8}	2.54×10^{8}	5.93×10^{8}
k_{-23} (i15→i3)	4.30×10^{11}	4.30×10^{11}	4.33×10^{11}	4.78×10^{11}	5.48×10^{11}	6.56×10^{11}
k_{24} (i3→i17)	6.20×10^{6}	6.27×10^{6}	6.59×10^{6}	1.35×10^{7}	3.60×10^{7}	1.32×10^{8}
k_{-24} (i17→i3)	2.41×10^{12}	2.42×10^{12}	2.46×10^{12}	3.05×10^{12}	3.99×10^{12}	5.48×10^{12}
k_{25} (i3→i14)	7.12×10^{7}	7.19×10^{7}	7.46×10^{7}	1.28×10^{8}	2.73×10^{8}	7.78×10^{8}
k_{26} (i3→i15′)	⋯	⋯	⋯	6.25×10^{2}	2.03×10^{4}	4.76×10^{5}
k_{-26} (i15′→i3)	⋯	⋯	⋯	1.27×10^{11}	1.13×10^{12}	5.09×10^{12}

[a]Computed with zero-point energy corrected B3LYP/6-311G(d,p) energies.

(c1→i4) and k_2 (c1→c2) being 7.10×10^{12} and 5.59×10^{11} s^{-1}, respectively, while the 3.54×10^{7} and 9.11×10^{4} s^{-1} of k_3 (c1→i5) and k_4 (c1→i9) are decidedly negligible. Thus, c1 is most likely to arrive at the two immediate intermediates, c2 and i4. As discussed in the section that follows, c2 would in fact prefer ring closing back to c1, which suggests the fate of c1 eventually depends solely on the chained i4, the most energetically stable intermediate.

Likely low energy paths for i4 could include 1,2 H-shift to c2, three-member ring closing back to c1, four-member ring closing to cyclobut-1,2,3-triene-1-ylidene-hydrocarbene (i11) at −18.6 kcal/mol, channel to five-member ringed cyclopent-1,3-diyl-1,2,4-triene (i6) at −34.9 kcal/mol, and hydrogen dissociating to p1+H of energy −9.6 kcal/mol. While attempts failed in finding tsc2i4, all other i4 transition states are located, of which the barriers are 53.1, 82.6, 90.2, and 95.2 kcal/mol for tsc1i4, tsi4i11, tsi4i6, and tsi4p1, respectively. With the lowest barrier, the i4→c1 channel is expected to be the most kinetically favored as well, which is ratified by the magnitude of computed rate constant k_{-1}, 7.98×10^{8} s^{-1} at 0 collision energy. In the order of decreasing kinetic competitiveness, k_1 is then surprisingly followed by k_{14} (i4→i11), k_{10} (i4→p1+H), and k_{13} (i4→i6), being 4.48×10^{3}, 1.51×10^{3}, and 8.56×10^{1} s^{-1}, respectively. The position of i4→p1+H is advanced owing to a particularly loose transition state, which dominates even more as the collision energy gets higher.

Accordingly, i4 would initially be guided by the minimum energy path to c1 which rushes right back to i4 as discussed above. The accumulated amount of i4 could only

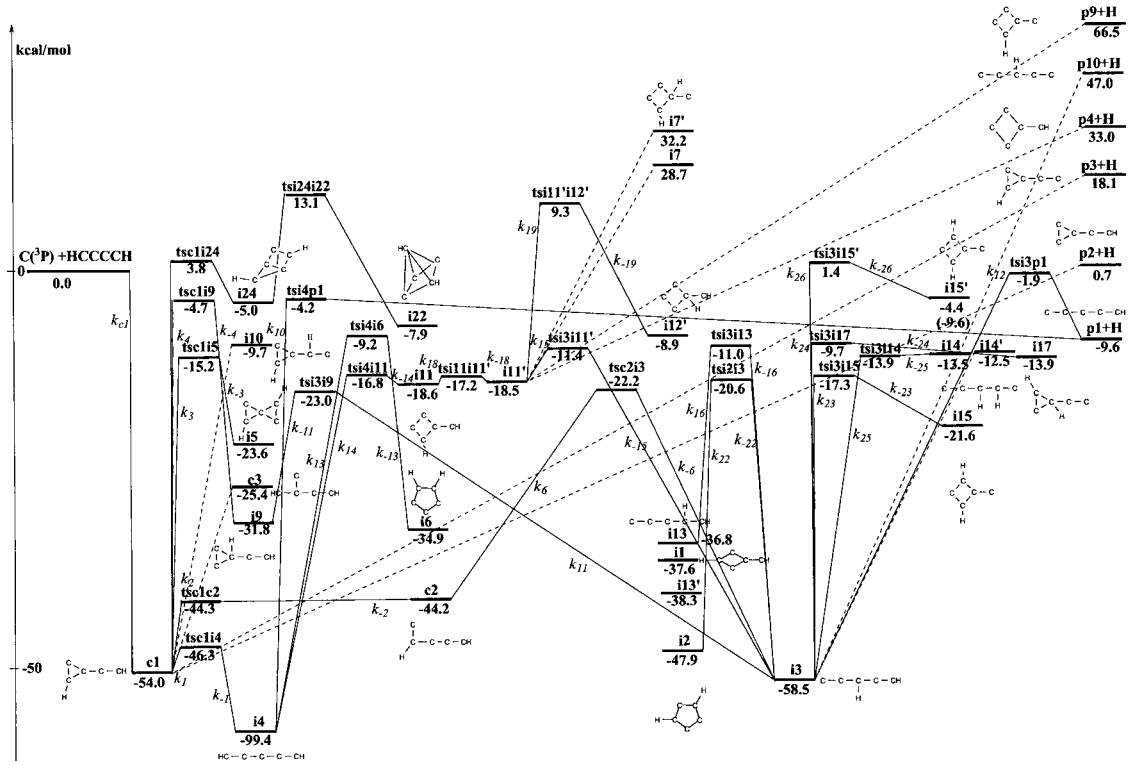

FIG. 5. The reaction paths of the collision complex c1, in which the energies in kcal/mol relative to the reactants, $C(^3P)+HCCCCH(X\ ^1\Sigma_g^+)$, are computed with CCSD(T)/cc-pVTZ level of theory with B3LYP/6-311G(d,p) zero-point energy corrections at the B3LYP/6-311G(d,p) optimized geometries as shown in Figs. 1–3. Note the attempts are not made to locate the transition states for those paths in dotted lines, unless otherwise stated in text.

look for seemingly unfavorable paths to p1 and i11 for dissipation. Of the four possible i11 ring openings, only two appear to be feasible as predicted by present level of computations, namely, i4 and but-1-yne-3-eneylidenecarbene (i3); the transition state for i11 H shifting to 1,3-butdiyn-3-ylidene-3-yne-carbene (i1) has not been obtained. Among the probable low energy channels of i11, k_{14} and k_{15} of 6.92×10^{12} and 9.24×10^{11} s^{-1} for the ring openings i11→i4 and

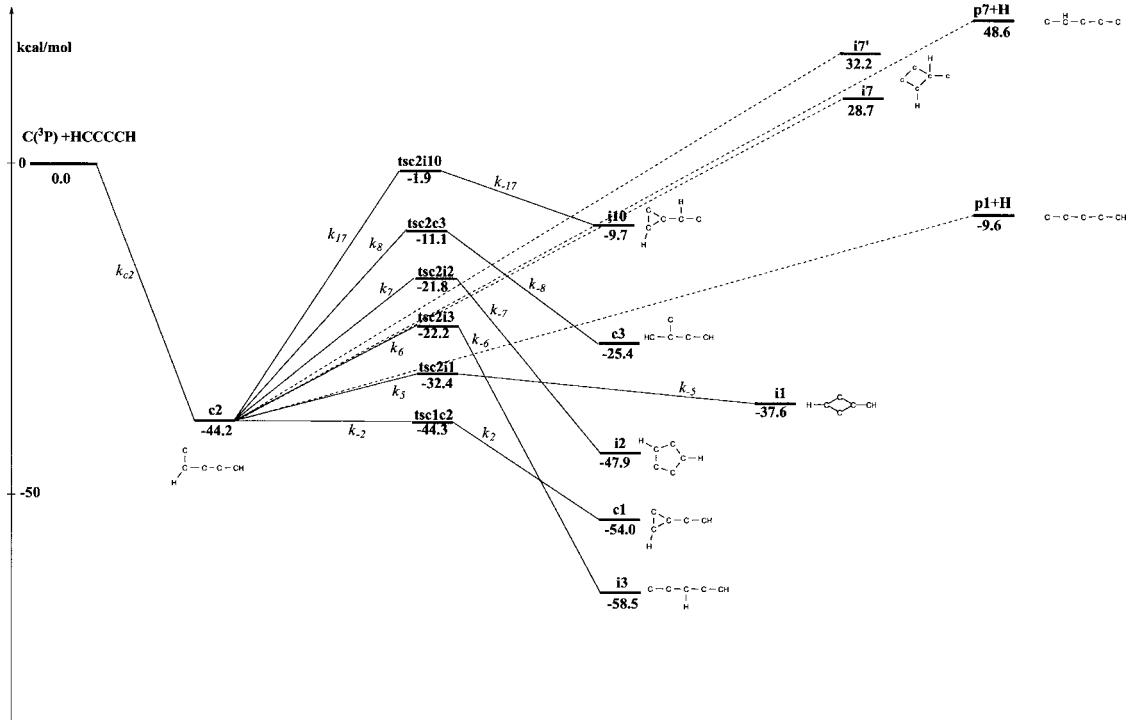

FIG. 6. The reaction paths of the collision complex c2, in which the energies in kcal/mol relative to the reactants, $C(^3P)+HCCCCH(X\ ^1\Sigma_g^+)$, are computed with CCSD(T)/cc-pVTZ level of theory with B3LYP/6-311G(d,p) zero-point energy corrections at the B3LYP/6-311G(d,p) optimized geometries as shown in Figs. 1–3. Note the attempts are not made to locate the transition states for those paths in dotted lines, unless otherwise stated in text.

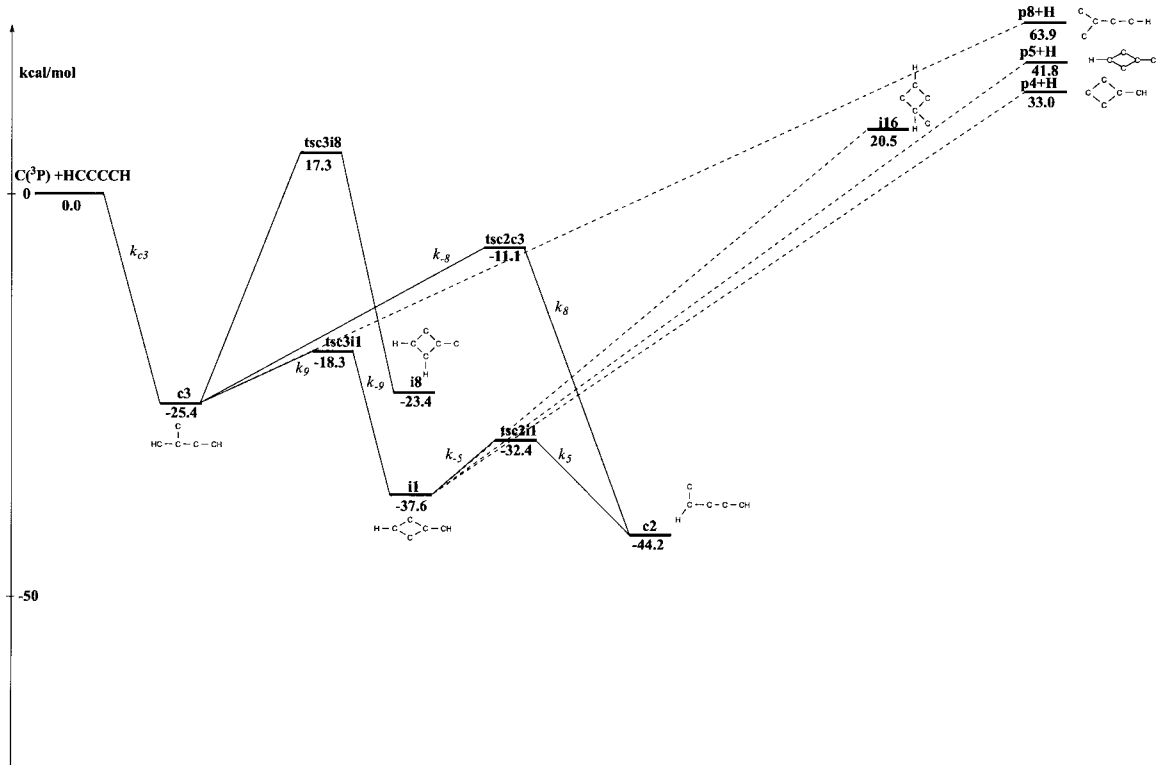

FIG. 7. The reaction paths of the collision complex c3, in which the energies in kcal/mol relative to the reactants, $C(^3P)+HCCCCH(X\ ^1\Sigma_g^+)$, are computed with CCSD(T)/cc-pVTZ level of theory with B3LYP/6-311G(d,p) zero-point energy corrections at the B3LYP/6-311G(d,p) optimized geometries as shown in Figs. 1–3. Note the attempts are not made to locate the transition states for those paths in dotted lines, unless otherwise stated in text.

i11→i3, respectively, have a clear advantage over two H-shifting reactions to i7 and bicyclo[1,1,0]but-1,2-diene-4-ylcarbene (i12), and two H dissociations to p4 and p9. It turns out that i3 has plenty of routes to proceed: three H-shifts to c2, E-pent-1,4-diene-3-yne-1-yl-5-ylidene (i13), and pent-1-yne-2,4-diene-1,5-diylidene (i14), ring formations to five-member ringed cyclopent-1-diyl-2,3,4-triene (i2), four-member ringed i11 and cyclobut-2,3-diene-1-ylidenecarbene (i15), i9 and 1-hydrogencycloprop-2-enyl-3-ylideneethynylidene (i17) of three-member ring, and H eliminations to p1 and p10. Compared with the next fastest k_{11} $(1.94\times10^9\ s^{-1})$ for i3→i9, rate constant calculations identify that i3→c2 with k_6 being $3.56\times10^{10}\ s^{-1}$ stands out as the most likely path, which simply takes c2 all the way back to i4. In another words, i4 would in fact seek to leak through the channel of p1+H.

D. Reaction paths of pent-4-ene-5, 5-diyl-1, 2-diyne (c2)

With the exception of the four-member ringed i7, the transition states to the possible c2 ring-formation isomers, the three-member ringed c1 and i10, four-member ringed i1, and the five-member ringed i2, are characterized as revealed in Fig. 6. Of three 1,2 H migrations, the tsc2i3 is the only transition state identified, with the activation energy computed to be 22.0 kcal/mol. The carbon migration converts c2 to fellow complex c3; dissociation channels could be carbon decomposition to reactants C+HCCCCH and H elimination to the chained p1 and p7.

Notably, the energy of c2, −44.2 kcal/mol, is higher than the −44.3 kcal/mol of tsc1c2, an indication that c2 is unstable with respect to the ring closing to c1. Thus, despite that there are at least six channels open and the most stable isomer is, in fact, i3, c2 seems inevitably converting to c1 immediately and assumes the c1 paths.

E. Reaction paths of 2-ethynyl-allene-1-yl-3-ylidene (c3)

The tsc3i8 for c3 ring closure to cyclobut-1-yne-3-ene-1-ylidenecarbene (i8) are at 17.3 kcal/mol and a H-dissociation product, p8, is much higher at 63.9 kcal/mol, while the transition state to c1, the isomers as a result of 1,2 H shift, and another H-dissociation product have not been located at this level of calculations. It appears merely three channels are found open to c3 at low temperature. As depicted in Fig. 7, the four-member ring formation to i1, carbon shift to produce c2, and carbon dissociation to reactants, are of the transition states, tsc3i1, tsc2c3, and tsc3, at −18.3, −11.1, and −1.1 (at 0 collision energy) kcal/mol and corresponds to rate constants, k_9, k_8, and k_{c3}, estimated as 4.79×10^{10}, 3.95×10^9, and $2.93\times10^6\ s^{-1}$, respectively. Being on the minimum energy path, i1 edges out as an evident immediate destination and subsequently dictates the fate of c3. Probable channels to consume i1 include two possible 1,2 H-shift reactions to i11 and i16, possible H dissociations to p4 and p5, and ring breakings to c3 and c2. The latest, i1→c2, suppresses others by virtue of much lower barrier. From this point on, the paths of c2 would be pursued.

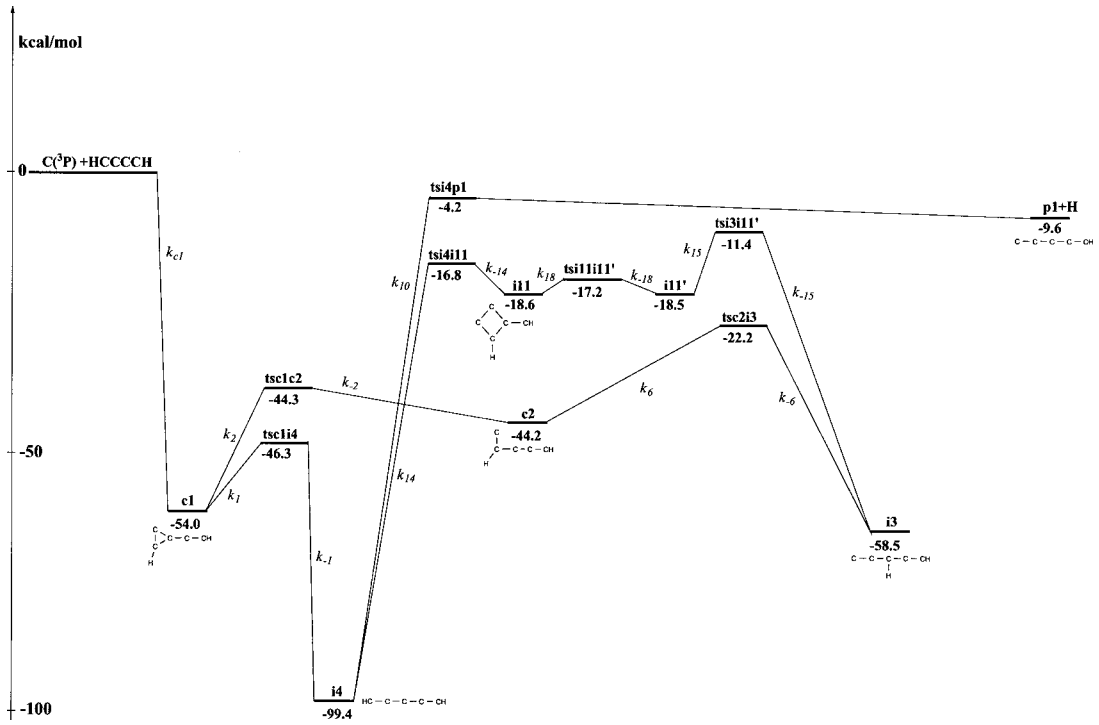

FIG. 8. The most probable paths of the collision complex c1, in which the energies in kcal/mol relative to the reactants, $C(^3P)+HCCCCH(X\,^1\Sigma_g^+)$, are computed with CCSD(T)/cc-pVTZ level of theory with B3LYP/6-311G(d,p) zero-point energy corrections at the B3LYP/6-311G(d,p) optimized geometries as shown in Figs. 1–3.

F. The most probable paths of collision complexes

The most probable paths of c1 are presented in Fig. 8 which are determined on the basis of the kinetic competitiveness at zero collision energy, simply, the paths with the largest rate constants but not necessarily the minimum energy paths. In Fig. 11(a), as Fig. 8 derived c1 reaction mechanism demonstrates, via two lowest energy paths with comparable rates, c1 would prefer ring opening to its immediate intermediates c2 and i4. While c2 goes back to c1, i4 could skip a

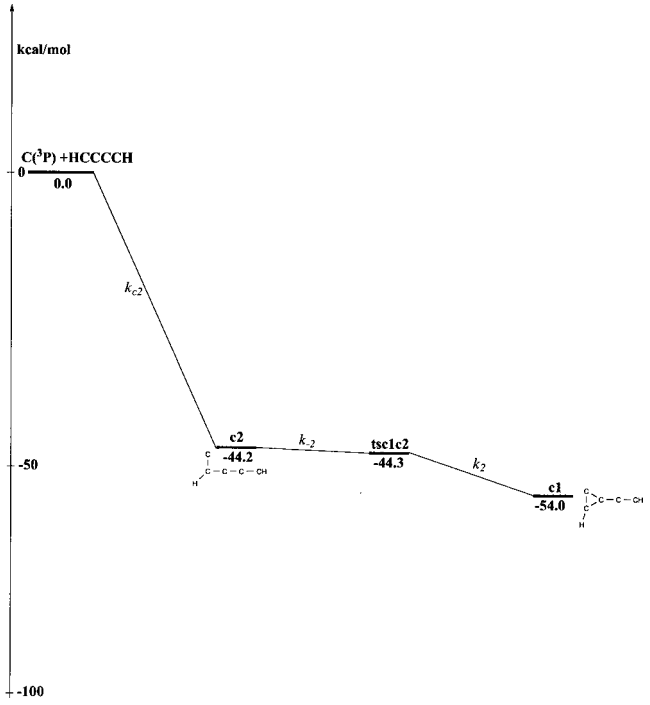

FIG. 9. The most probable paths of the collision complex c2, in which the energies in kcal/mol relative to the reactants, $C(^3P)+HCCCCH(X\,^1\Sigma_g^+)$, are computed with CCSD(T)/cc-pVTZ level of theory with B3LYP/6-311G(d,p) zero-point energy corrections at the B3LYP/6-311G(d,p) optimized geometries as shown in Figs. 1–3.

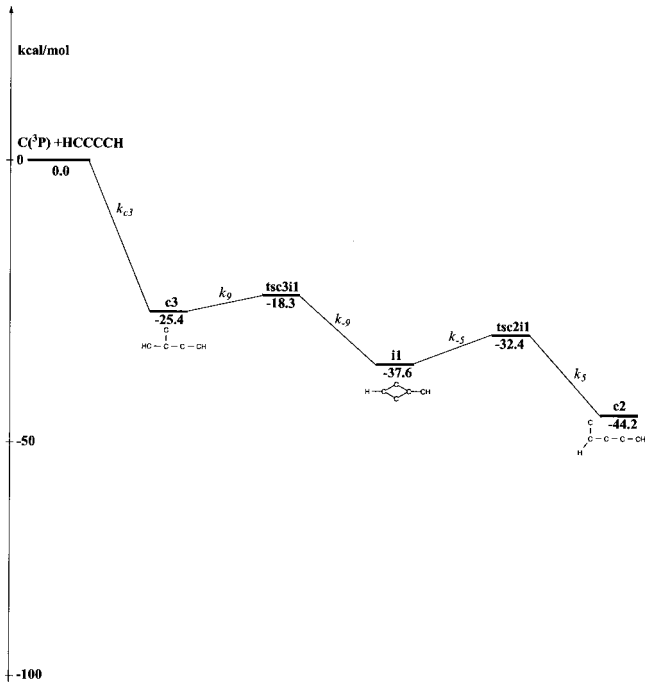

FIG. 10. The most probable paths of the collision complex c3, in which the energies in kcal/mol relative to the reactants, $C(^3P)+HCCCCH(X\,^1\Sigma_g^+)$, are computed with CCSD(T)/cc-pVTZ level of theory with B3LYP/6-311G(d,p) zero-point energy corrections at the B3LYP/6-311G(d,p) optimized geometries as shown in Figs. 1–3.

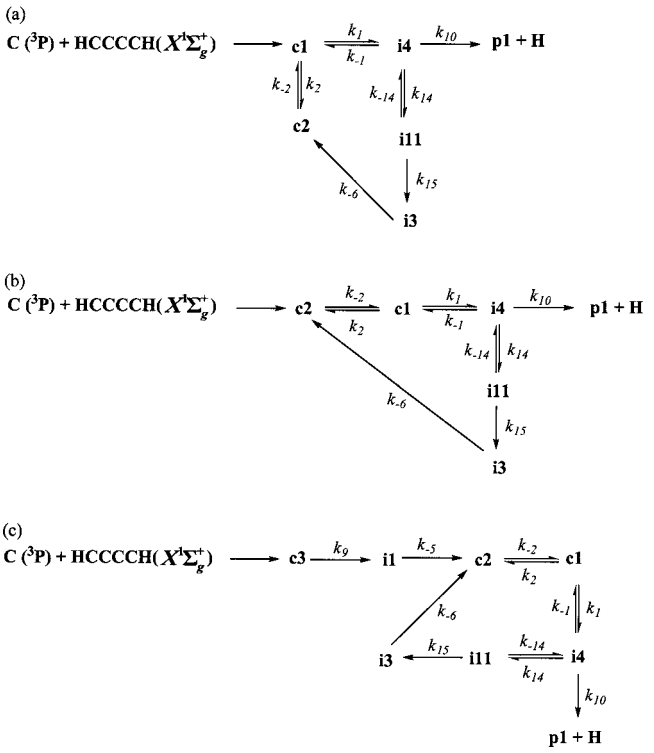

FIG. 11. The reaction mechanisms (a–c) derived from the most probable paths of collision complexes (c1–c3), respectively, in which the k's are the corresponding rate constants.

relatively energetically favored path to i6 and proceed through three channels to c1, i11, and p1. With two least hindered pathways, cyclic i11 easily stretches to yield chain i4 again and i3. i3 bypasses the minimum energy path to ringed i9 and chooses a more efficient way out instead, by H shifting to c2. The (c1, i4) loop could break away only by means of i4 H dissociation to the exclusive product p1.

The c2 minimum energy path to c1 is comfortably the most probable, as shown in Fig. 9. c2 reaction mechanism thus inferred in Fig. 11(b) should closely resemble c1's. Likewise, as laid out in Fig. 10, the most probable immediate path of c3 is at the same time the minimum energy path which guides c3 to the four-member ringed i1 and, right afterwards, c2. Accordingly, the corresponding mechanism in Fig. 11(c) illustrates that the same (c1, i4) route would usher c3 all the way to the only product available, p1.

It is worth noting that the paths presented in Figs. 8–10 are marked energetically, their complementary [Figs. 11(a)–11(c)] could give a clear indication for the direction of reaction.

G. Evolution of concentrations with time

The rate equations derived from mechanisms of C +HCCCCH reaction via c1, c2, and c3 as seen in Figs. 11(a)–11(c), respectively, are set up; these three sets of simultaneous differential equations in 6, 6, and 8 unknown concentrations, respectively, are then solved numerically, in which the RRKM rate constants of Table I are adopted. The evolution of concentrations with time thus obtained at collision energies of 0 for each species in the three reaction mechanisms are shown in Figs. 12–14 at collision energy 10 kcal/mol, those of c1 mechanism are presented in Fig. 12, while those of c2 and c3 are revealed in Fig. s2.[73]

As illustrated in Fig. 12, for the C+HCCCCH proceeding through collision complex c1 with the condition that initially (t=0) there is only c1, c1 simply dies down after a fraction of a picosecond as its immediate isomers, c2 and i4, rise up at the same time. While c2 amounts to a small but non-negligible ~0.05 of c1 initial concentration with a lifetime in picoseconds, the peak i4 reaches 1.0 and persists well into milli- and microseconds for collision energy of 0 and 10 kcal/mol, respectively. The lifetimes of i4 reflect appropriately the magnitudes of its bottle-neck rate constants k_{10} of i4→p1+H, 1.51×10^{3} and 1.13×10^{6} s^{-1} at these two collision energies. The instant when i4 is formed, the detouring to i11 takes off such that the rise and fall of i4 and i11 are almost synchronized in time, as seen in Fig. 12. At any moment during reaction, a $k_{14}/(k_{-1}+k_{10}+k_{14})$ portion of i4 could yield i11, which reduces to a mere 5.6×10^{-6} at 0 collision energy even when i4 is 1.0 in concentration. Compounded by the fact that i11 dissipating rate constants, k_{14} and k_{15}, are overwhelmingly larger than the only buildup rate constant k_{14}, i11 drains instantly and does not have a chance to accumulate as indicated by the dismal maximum concentration, around 10^{-10}. With i11 being its single source, i3 is not expected to pile up to any significant quantity; however, due to a slower dissipating step to c2 (k_{-6}) than building up out of i11 (k_{15}), i3 does acquire a higher peak concentration than i11's. i4 leaking to the only products, p1+H, or equivalently, the formation of p1, takes milliseconds and microseconds to complete at collision energy of 0 and 10 kcal/mol, respectively, which also marks the end of the reaction at a single-collision environment. It is particularly interesting to note that for a typical detection time of microseconds in crossed beam experiments, the results indicate the intermediate i4 can be captured at near zero collision energy. Intermediates and product peak earlier and attain higher maximum concentrations at collision energy of 10 kcal/mol than at 0 kcal/mol, with obvious exception of i4 and p1 whose peak concentrations remain at 1.0.

For the bimolecular reaction by way of collision complex c2 seen in Figs. 13 and s2(a), c2 could disappear around 1 ps given the ring closure k_{-2} (c2→c1) being $1.89-1.92\times10^{12}$ s^{-1}. Now that c1 acts as the immediate intermediate of c2, the rest of the species in loop (c1, i4) have a time delay in reaching the same peak concentrations compared with mechanism c1 in Fig. 12. Otherwise, unsurprisingly the concentration evolutions in c2 mechanism share the same features as in c1's.

Intriguingly, the mechanism c3 in Fig. 14 and s2(b) demonstrates that the least energetically stable collision complex c3, however, lasts longer than c1 and c2 in Figs. 12 and 13 respectively, and has a lifetime of ten to twenty picoseconds as estimated from the inverse of k_9. The moment its immediate intermediate i1 is formed, the ring opening to c2 takes place; thus the peak concentration of i1 only reaches around 10^{-3} of the c3 initial concentration. When the reaction proceeds to c2, the routes of c2 mechanism, as in Fig. 11(b), are then followed.

While all other species in the predicted mechanisms

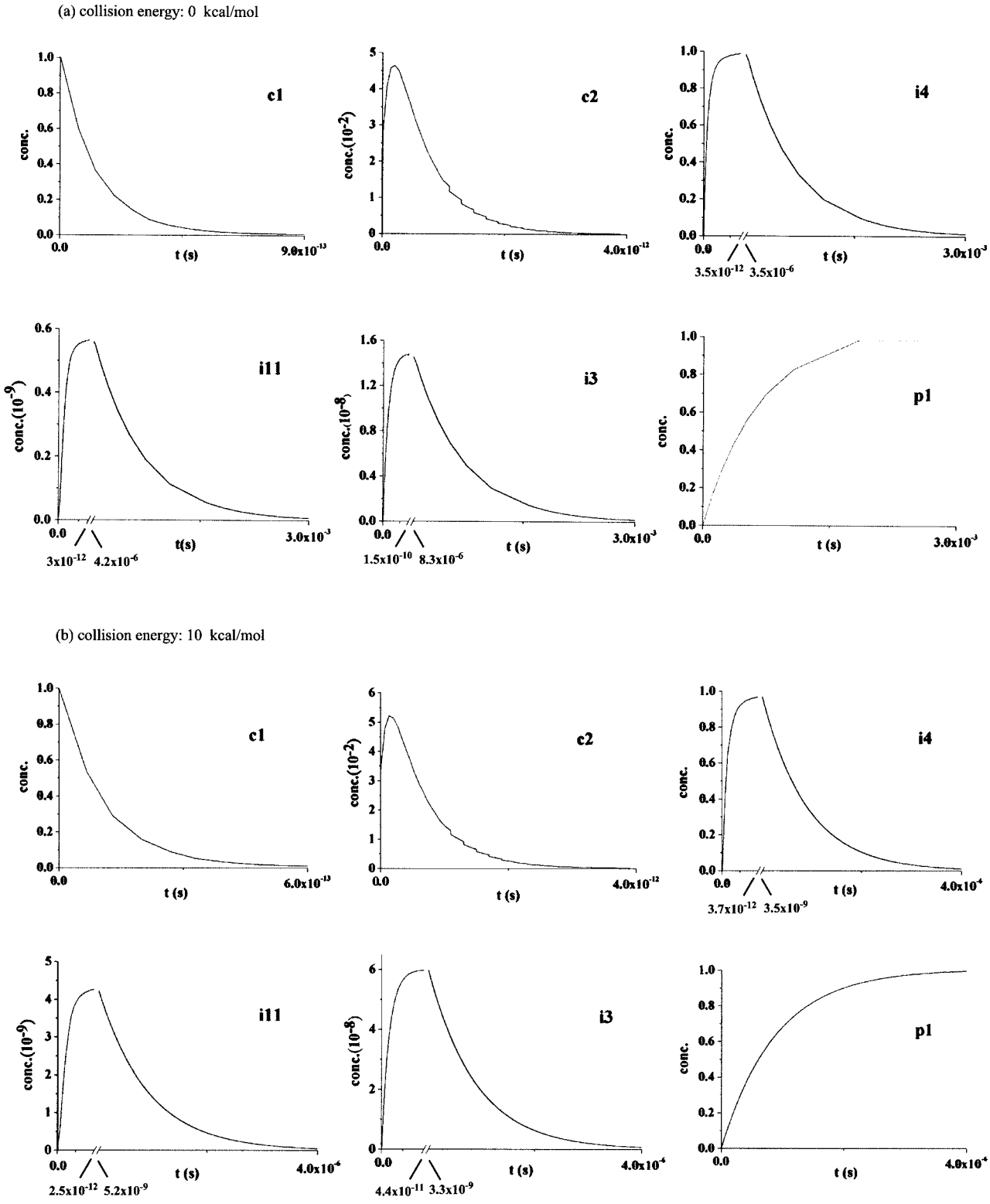

FIG. 12. The evolution of concentration with time for each species in c1 reaction mechanism as in Fig. 11(a) at collision energies of (a) 0 and (b) 10 kcal/mol.

would be elusive for detection with perhaps an exception of p1, i4 remains the easiest target to trap for its duel roles of both intermediate and product due to a long lifetime within collision energy of 0–10 kcal/mol. For a typical detection time scale of a microsecond in crossed beam experiment, our results give a mixture of i4 and p1 with 1:2 ratio at 10 kcal/mol and i4 as an exclusive product at 0 collision energy.

The $\sigma_{c1}:\sigma_{c2}:\sigma_{c3}$ is estimated to be practically 1:1:1, which implies that the overall reaction mechanism for $C(^3P)+HCCCCH(X\,^1\Sigma_g^+)$ is consisted of three equally weighted mechanisms as laid out in Fig. 11.

H. Assessing the branching ratio of i3→p1+H

Note that i3→p1+H is left out of the most probable outgoing paths for i3, thus excluded from the reaction

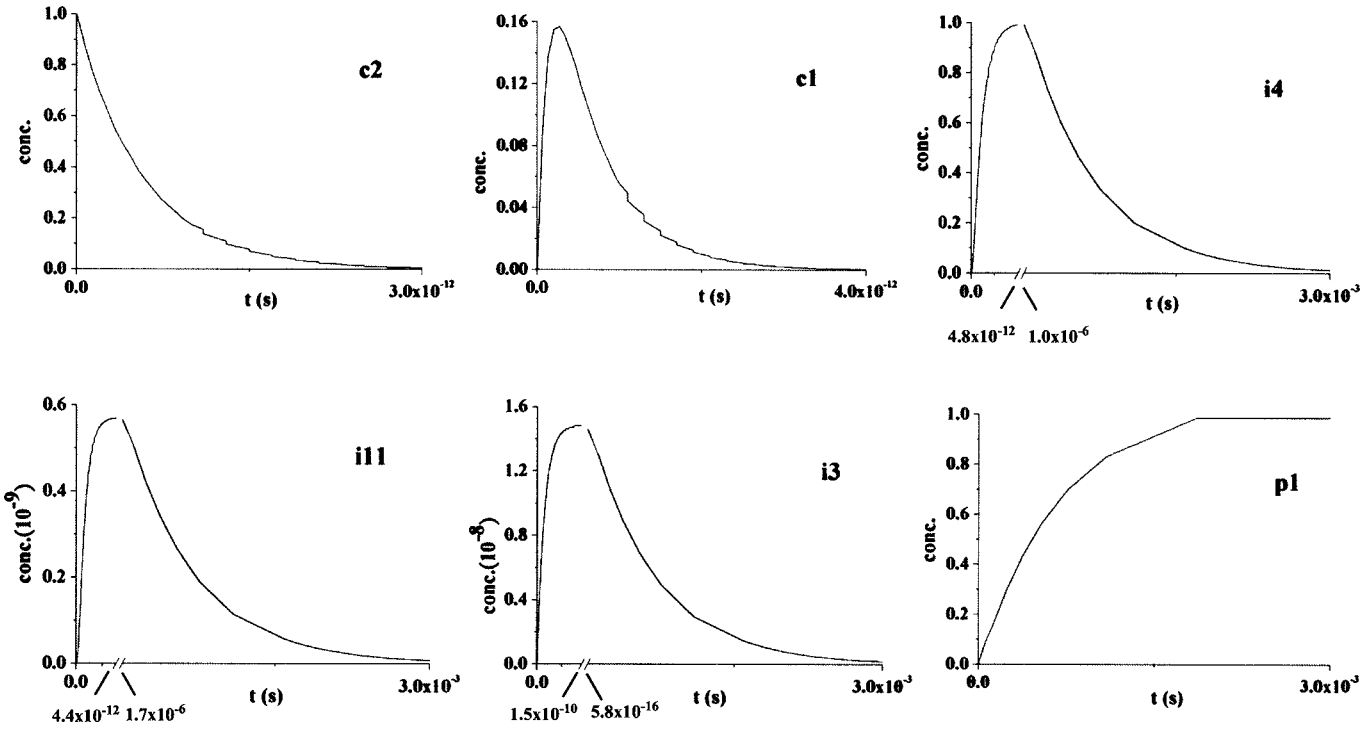

FIG. 13. The evolution of concentration with time for each species in c2 reaction mechanism as in Fig. 11(b) at zero collision energy.

mechanism due to its much smaller rate constant k_{12} (4.83×10^4 s^{-1}) compared with the k_{-6}(3.56×10^{10} s^{-1}) of i3 $\rightarrow$c2, while the seemingly unlikely i4$\rightarrow$p1+H with a 30 fold smaller k_{10} (1.51×10^3 s^{-1}) has been firmly put in the reaction mechanism. The validity of present scheme for identifying the most probable paths, thus reaction mechanism, could be nicely demonstrated by estimating the branching ratio of i3$\rightarrow$p1+H vs. i4$\rightarrow$p1+H. In order to incorporate i3$\rightarrow$p1+H channel, the seven more efficient i3 outgoing paths to i9, i2, i13, i15, i14, i11′, and i17 are also included,

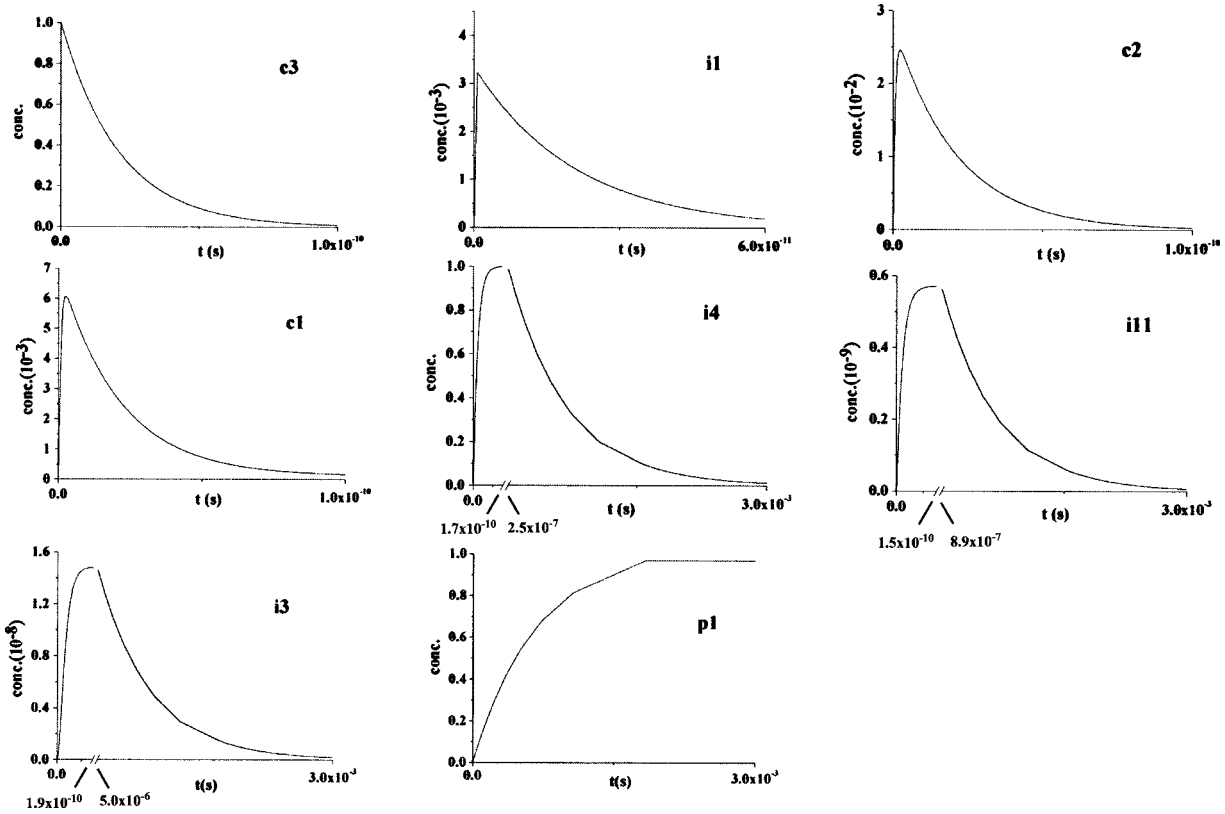

FIG. 14. The evolution of concentration with time for each species in c3 reaction mechanism as in Fig. 11(c) at zero collision energy.

their immediate reaction paths and rate constants further scrutinized as detailed in Figs. s3 and s4 and Table sII.[73] The c1 mechanism eventually adapted for this task is depicted in Fig. s2, along with the corresponding plots of concentration versus time at 10 kcal/mol. The branching ratio for i3 $\rightarrow$p1+H:i4$\rightarrow$p1+H is predicted to be 4×10^{-6}:1. It indicates that the channel of i3$\rightarrow$p1+H is indeed negligible and i4 is the sole provider for the exclusive product p1. The demonstration lands support to our kinetic scheme.

I. Notes on C_5H_2 isomers

Relevant C_5H_2 isomers identified in this work sum up to an impressive 38, as paraded in Figs. 1, 2, and s4, the optimized structures for three collision complexes and 35 intermediates. Among them, six isomers have previously been predicted at various levels of theory, specifically, the singlet c1,[48,51,52] i3,[49,51] i4,[48,49] i18,[51] i20,[48,49,51,56] and triplet c1,[52] c3,[52] i3,[49] i4,[49–55] i20,[49] which leaves the number of newly found C_5H_2 isomers being 32.

IV. CONCLUSION

The important interstellar reaction of the ground state carbon atom, $C(^3P)$, with carbon chain diacetylene, HCCCCH($X\,^1\Sigma_g^+$), has been investigated by employing *ab initio* electronic structure calculations for predicting reaction paths, subsequently RRKM theory to yield rate constants at six collision energies for each path, and a modified Langevine model for estimating capturing cross sections. By combining these results, the most probable paths are identified and adopted as the reaction mechanism of which the rate equations are solved numerically such that the evolutions of concentrations with time are obtained.

Three collision complexes, c1, c2, and c3, without entrance barrier, 35 relevant intermediates, and 10 H-dissociated products are located. Overall, 32 C_5H_2 and two C_5H isomers are newly found in this work.

This study predicts that three collision complexes, c1, c2, and c3, would end up at one single final product, linear C_5H (p1)+H, via the most stable intermediate, linear HC_5H (i4). That is while the first member of interstellar reaction class, $C(^3P)+C_2H_2\rightarrow C_3H+H$, is famously known to form both linear and cyclic C_3H isomers with the latter being lower in energy, the second member $C(^3P)+HC_4H\rightarrow C_5H+H$ is found to produce only the carbon chain C_5H, the most stable isomer. Our investigation indicates that the $C(^3P)+$HCCCCH($X\,^1\Sigma_g^+$) reaction would be efficient route for diacetylene depletion and 2,4-pentadiynylidyne, HCCCCC($X\,^2\Pi$), formation in interstellar medium. This is in strong contrast to the reaction of tricarbon, $C_3(X\,^1\Sigma_g^+)$, with acetylene, HCCH($X\,^1\Sigma_g^+$). Here,[74] although the 2,4-pentadiynylidyne, HCCCCC($X\,^2\Pi$), isomer was identified as a product under single collision conditions, this reaction was found to be strongly endoergic by about 24 kcal/mol. Therefore, the barrierless and exoergic reaction of ground state carbon atoms with diacetylene presents a compelling route to synthesize 2,4-pentadiynylidyne, HCCCCC($X\,^2\Pi$), in cold molecular clouds.

ACKNOWLEDGMENTS

Computer resources at the National Center for High-Performance Computer of Taiwan were utilized in the calculations.

[1] H. S. P. Muller, S. Thorwirth, D. A. Roth, and G. Winnerwisser, Astron. Astrophys. **370**, L49 (2001); http://www.cdms.de
[2] M. B. Bell, P. A. Feldman, M. J. Travers, M. C. McCarthy, C. A. Gottlieb, and P. Thaddeus, Astrophys. J. **483**, L61 (1997).
[3] O. E. H. Rydbeck, J. Ellder, and W. M. Irvine, Nature (London) **246**, 466 (1973).
[4] K. D. Tucker, M. L. Kutner, and P. Thaddeus, Astrophys. J. **193**, L115 (1974).
[5] P. Thaddeus, C. A. Gottlieb, A. Hjalmarson, L. E. B. Johannson, W. M. Irvine, P. Friberg, and R. A. Linke, Astrophys. J. **294**, L49 (1985).
[6] M. Guelin, S. Green, and P. Thaddeus, Astrophys. J. **224**, L27 (1978).
[7] J. Cernicharo, C. Kahane, J. Gomez-Gonzalez, and M. Guelin, Astron. Astrophys. **164**, L1 (1986).
[8] H. Suzuki, M. Ohishi, N. Kaifu, S. I. Ishikawa, and T. Kasuga, Publ. Astron. Soc. Jpn. **38**, 911 (1986).
[9] M. Guelin, J. Gernicharo, M. J. Travers, M. C. McCarthy, C. A. Gottlieb, P. Thaddeus, M. Ohishi, S. Saito, and S. Yamamoto, Astron. Astrophys. **317**, L1 (1997).
[10] J. Cernicharo and M. Guelin, Astron. Astrophys. **309**, L27 (1996).
[11] J. Cernicharo, A. M. Heras, A. G. G. M. Tielens, J. R. Pardo, F. Herpin, M. Guelin, and L. B. F. M. Waters, Astrophys. J. **546**, L123 (2001).
[12] B. E. Turner, Astrophys. J. **163**, L35 (1971).
[13] M. Morris, W. Gilmore, P. Palmer, B. E. Turner, and B. Zuckerman, Astrophys. J. **199**, L47 (1975).
[14] N. W. Broten, T. Oka, L. W. Avery, J. M. MacLeod, and H. W. Kroto, Astrophys. J. **223**, L105 (1978).
[15] H. W. Kroto, C. Kirby, D. R. M. Walton, L. W. Broten, J. M. MacLead, and T. Oka, Astrophys. J. **219**, L133 (1978).
[16] J. Cernicharo, C. A. Gottlieb, M. Guelin, T. C. Killian, G. Paubert, P. Thaddeus, and J. M. Vrtilek, Astrophys. J. **368**, L39 (1991).
[17] J. Cernicharo, C. A. Gottlieb, M. Guelin, T. C. Killian, P. Thaddeus, and J. M. Vrtilek, Astrophys. J. **368**, L43 (1991).
[18] W. D. Langer, T. Velusamy, T. B. H. Kuiper, R. Peng, M. C. McCarthy, M. J. Travers, A. Kovacs, C. A. Gottlieb, and P. Thaddeus, Astrophys. J. **480**, L63 (1997).
[19] G. H. Herbig, Annu. Rev. Astron. Astrophys. **33**, 19 (1995).
[20] A. E. Douglas, Nature (London) **269**, 130 (1977).
[21] J. Fulara, D. Lessen, P. Frelvogel, and J. P. Maier, Nature (London) **366**, 439 (1993).
[22] M. Tulej, D. A. Kirkwood, M. Pachkov, and J. P. Maier, Astrophys. J. **506**, L69 (1998).
[23] B. J. McCall, J. Thorburn, L. M. Hobbs, T. Oka, and D. G. York, Astrophys. J. **559**, L49 (2001).
[24] G. Galazutdinov, F. Musaev, J. Nirski, and J. Krelowski, Astron. Astrophys. **377**, 1063 (2001).
[25] T. Allain, S. Leach, and E. Sedlmayr, Astron. Astrophys. **305**, 602 (1995).
[26] J. P. Maier, J. Phys. Chem. A **102**, 3462 (1998).
[27] M. L. Heger, Lick Obs. Bull. **10**, 146 (1922).
[28] T. Pinto, H. Ding, F. Guthe, and J. P. Maier, J. Chem. Phys. **114**, 2208 (2001).
[29] C. D. Ball, M. C. McCarthy, and P. Thaddeus, Astrophys. J. **523**, L89 (1999).
[30] C. D. Ball, M. C. McCarthy, and P. Thaddeus, J. Chem. Phys. **112**, 10149 (2000).
[31] H. Ding, T. W. Schmidt, T. Pinto, A. E. Boguslavskiy, F. Guthe, and J. P. Maier, J. Chem. Phys. **119**, 814 (2003).
[32] M. Kotterer and J. P. Maier, Chem. Phys. Lett. **266**, 342 (1997).
[33] H. Linnartz, T. Motylewski, O. Vaizert, J. P. Maier, A. J. Apponi, M. C. McCarthy, C. A. Gottlieb, and P. Thaddeus, J. Mol. Spectrosc. **197**, 1 (1999).
[34] H. Linnartz, T. Motylewski, and J. P. Maier, J. Chem. Phys. **109**, 3819 (1998).
[35] H. Ding, T. Pino, F. Guthe, and J. P. Maier, J. Chem. Phys. **117**, 8362 (2002).
[36] K. Hoshina, H. Kohguchi, Y. Ohshima, and Y. Endo, J. Chem. Phys. **108**, 3465 (1998).
[37] A. Dzhonson, E. B. Jochnowitz, E. Kim, and J. P. Maier, J. Chem. Phys.

126, 044301 (2007).
[38] E. Herbst, H. H. Lee, D. A. Howe, and T. J. Millar, Mon. Not. R. Astron. Soc. **268**, 335 (1994).
[39] R. P. Bettens, H. H. Lee, and E. Herbst, Astrophys. J. **443**, 664 (1995).
[40] R. P. Bettens and E. Herbst, Astrophys. J. **468**, 686 (1996).
[41] T. J. Millar, P. R. A. Farquhar, and K. Willacy, Astron. Astrophys. **121**, 139 (1997).
[42] E. Herbst, Chem. Soc. Rev. **30**, 168 (2001).
[43] R. I. Kaiser, Chem. Rev. (Washington, D.C.) **102**, 1309 (2001).
[44] R. I. Kaiser, C. Ochsenfeld, M. Head-Gordon, and Y. T. Lee, Science **274**, 1508 (1996).
[45] D. C. Clary, E. Buonomo, I. R. Sims, I. W. M. Smith, W. D. Geppert, C. Naulin, M. Costes, L. Cartechini, and P. Casavecchia, J. Phys. Chem. A **106**, 5541 (2002), and the references therein.
[46] M. C. McCarthy, M. J. Travers, A. Kovacs, W. Chen, S. E. Novick, C. A. Gottlieb, and P. Thaddeus, Science **275**, 518 (1997).
[47] M. C. McCarthy, M. J. Travers, A. Kovacs, C. A. Gottlieb, and P. Thaddeus, Astrophys. J., Suppl. Ser. **113**, 105 (1997).
[48] D. L. Cooper and S. C. Murphy, Astrophys. J. **333**, 482 (1988).
[49] S. J. Blanksby, S. Dua, J. H. Bowie, D. Schroder, and H. Schwarz, J. Phys. Chem. A **102**, 9949 (1998).
[50] Q. Fan and G. V. Pfeiffer, Chem. Phys. Lett. **162**, 472 (1989).
[51] R. A. Seburg, R. J. McMahon, J. F. Stanton, and J. Gauss, J. Am. Chem. Soc. **119**, 10838 (1997).
[52] J. Takahashi, Publ. Astron. Soc. Jpn. **52**, 401 (2000).
[53] A. Mavrandonakis, M. Muhlhauser, G. E. Froudakis, and S. D. Peyerimhoff, Phys. Chem. Chem. Phys. **4**, 3318 (2002).
[54] C. Zhang, Z. Cao, H. Wu, and Q. Zhang, Int. J. Quantum Chem. **98**, 299 (2004).
[55] N. P. Bowling, R. J. Halter, J. A. Hodges, R. A. Seburg, P. S. Thomas, C. S. Simmons, J. F. Stanton, and R. J. McMahon, J. Am. Chem. Soc. **128**, 3291 (2006).
[56] S. A. Maluendes and A. D. McLean, Chem. Phys. Lett. **200**, 511 (1992).
[57] F. Pauzat, Y. Ellinger, and A. D. McLean, Astrophys. J. **369**, L13 (1991).
[58] D. E. Woon, Chem. Phys. Lett. **244**, 45 (1995).
[59] S. J. Blanksby, S. Dua, and J. H. Bowie, J. Phys. Chem. A **103**, 5161 (1999).
[60] T. D. Crawford, J. F. Stanton, J. C. Saeh, and H. F. Schaefer, J. Am. Chem. Soc. **121**, 1902 (1999).
[61] J. Haubrich, M. Muhlhauser, and S. D. Peyerimhoff, J. Phys. Chem. A **106**, 8201 (2002).
[62] H. F. Su, R. J. Kaiser, and A. H. H. Chang, J. Chem. Phys. **122**, 074320 (2005).
[63] H. Y. Li, W. C. Cheng, Y. L. Liu, B. J. Sun, C. Y. Huang, K. T. Chen, M. S. Tang, R. I. Kaiser, and A. H. H. Chang, J. Chem. Phys. **124**, 044307 (2006).
[64] R. D. Levine and R. B. Bernstein, *Molecular Reaction Dynamics and Chemical Reactivity* (Oxford University Press, New York, 1987).
[65] A. D. Becke, J. Chem. Phys. **98**, 5648 (1993); **96**, 2155 (1992); **97**, 9173 (1992); C. Lee, W. Yang, and R. G. Parr, Phys. Rev. B **37**, 785 (1988).
[66] G. D. Purvis and R. J. Bartlett, J. Chem. Phys. **76**, 1910 (1982); C. Hampel, K. A. Peterson, and H.-J. Werner, Chem. Phys. Lett. **190**, 1 (1992); P. J. Knowles, C. Hampel, and H.-J. Werner, J. Chem. Phys. **99**, 5219 (1994); M. J. O. Deegan and P. J. Knowles, Chem. Phys. Lett. **277**, 321 (1994).
[67] M. J. Frisch *et al.*, GAUSSIAN 98, Revision A.5, Gaussian, Inc., Pittsburgh, PA, 1998; M. J. Frisch *et al.*, GAUSSIAN 03, Revision C.02, Gaussian, Inc., Wallingford, CT, 2004.
[68] H. Eyring, S. H. Lin, and S. M. Lin, *Basic Chemical Kinetics* (Wiley, New York, 1980).
[69] A. H. H. Chang, A. M. Mebel, X.-M. Yang, S. H. Lin, and Y. T. Lee, J. Chem. Phys. **109**, 2748 (1998).
[70] W. L. Hase, Acc. Chem. Res. **16**, 258 (1983).
[71] R. A. Marcus, Chem. Phys. Lett. **144**, 208 (1988).
[72] A. H. H. Chang, D. W. Hwang, X. M. Yang, A. M. Mebel, S. H. Lin, and Y. T. Lee, J. Chem. Phys. **110**, 10810 (1999).
[73] See EPAPS Document No. E-JCPSA6-128-012820 for the illustrations of Figs. s1, s2, and Table sI. For more information on EPAPS, see http://www.aip.org/pubservs/epaps.html.
[74] A. M. Mebel, G. S. Kim, V. V. Kislov, and R. I. Kaiser, J. Phys. Chem. A **111**, 6704 (2007); X. Gu, Y. Guo, A. M. Mebel, and R. I. Kaiser, Chem. Phys. Lett. **449**, 44 (2007).